INSTABILITY THRESHOLDS FOR FLEXIBLE ROTORS IN HYDRODYNAMIC BEARINGS

Paul E. Allaire and Ronald D. Flack
Department of Mechanical and Aerospace Engineering
University of Virginia
Charlottesville, Virginia 22903

ABSTRACT

Turbomachinery supported on hydrodynamic bearings may be either driven unstable or be stabilized by the bearing design. The purpose of this paper is to consider some designs for multilobe and pressure dam bearings in a flexible rotor. For non-optimized bearings, the correlation between theory and experiment is fairly good while for optimum designs it is not. A summary chart giving some of the advantages and disadvantages of various bearing types is also included.

NOMENCLATURE

Dimensional Quantities

c, c_1, c_2 = Bearing radial clearance, number one bearing, number two bearing (L)

c_b = Minimum film thickness for a centered shaft (L)

c_d = Step height (L)

c_p = Lobe clearance (L)

C_{xx}, C_{xy}, C_{yx}, C_{yy} = Bearing damping coefficients (FTL^{-1})

D = Bearing diameter (L)

e = Bearing eccentricity (L)

F_x, F_y = Bearing forces in the x and y directions (F)

g = Gravitational acceleration (L/T^2)

h_1, h_2 = Film thickness before, after step, centered bearing ($h_2 = c$) (L)

K_{xx}, K_{xy}, K_{yx}, K_{yy} = Bearing stiffness coefficients (FL^{-1})

K' = $\frac{h_1}{h_2} = \frac{h_1}{c}$, Film thickness ratio

L = Bearing length (L)

L_d, L_t = Step bearing axial dam length, relief track axial length (L)

m, m' = Rotor mass (M)

N, N_s = Shaft rotational speed (RPM), (RPS)

O_b, O_j, O_p = Bearing, journal, pad center

R = Radius of shaft (journal) (L)

R_p = Lobe radius (L)

W, W_T = Static bearing load (F)

x, y = Journal position in the x and y coordinates (L)

$\dot{x}, \dot{y}$ = Journal velocity in the x and y coordinates (L/T)

$\ddot{x}, \ddot{y}$ = Journal acceleration in the x and y coordinates (L/T^2)

γ_g = Groove location, (degrees)

δ = Pad tilt angle (degrees)

μ = Fluid viscosity (FT/L^2)

ω_d = Rotor whirl frequency (1/T)

ω_j = Journal rotational speed (1/T)

ω_r = Rotor critical speed on rigid support (1/T)

θ_g = Groove location, (degrees)

θ_s = Location of step measured with rotation from positive x-axis (degrees)

χ = Lobe arc length

Non-Dimensional Quantities

$\bar{L}_d, \bar{L}_t$ = L_d/L, L_t/L, Step bearing axial dam length ratio, relief track axial length ratio

m_1, m_2 = Preload in multilobe bearings

$\bar{M}$ = Rotor mass, $\omega_j{}^2 cm/W$

Re_2 = Reynolds number for step bearing

S = $\frac{\mu N_s LD}{W_T}\left(\frac{R}{c}\right)^2$, Sommerfeld number

S' = $\frac{\mu N_s LD}{W_T}\left(\frac{R}{c_b}\right)^2$, Sommerfeld number

η = Bearing parameter $\frac{S}{\bar{\omega}_j}\ \mu LD\left(\frac{D}{c}\right)^2\left(\frac{W}{cm}\right)^{1/2}/8\pi W$

$\bar{\omega}_d$ = Whirl frequency ratio, ω_d/ω_j

$\bar{\omega}_j$ = Rotor speed parameter, $\omega_j\sqrt{mc/W}$

ω_s = $\omega_j\sqrt{c/g}$, Rotor speed parameter, horizontal rotor

ω_s = $\omega_j\sqrt{\frac{mc}{W_T}}$, Rotor speed parameter

$\bar{\omega}_s$ = Rigid rotor stability threshold

$\bar{\bar{\omega}}_s$ = Flexible rotor stability threshold

α = Offset factor

ε = e/c_b, Bearing eccentricity ratio

Subscripts

b = Bearing

d = Dam

g = Groove

j = Journal

max = Maximum magnitude

p = Pad or lobe

r = Relative to equilibrium position

s = Step

t = Track

x,y = Horizontal and vertical directions

1,2 = Bearings 1 and 2 in experimental rotor

INTRODUCTION

Many of the bearings which are discussed in this paper have been developed principally to combat one or another of the causes of vibration. It is fortunate for designers of rotating machinery that a bearing which has good stiffness and damping properties such that it will suppress one of the causes of vibration will usually moderate one of the others as well. It should be noted, however, that the range of bearing properties due to the different geometric effects is so large that one must be relatively careful to choose the bearing with the proper characteristics for the particular causes of vibration for a given machine. In other words, there is no one bearing which will fix every machine.

It is often the case in industry that rotating machinery is primarily designed from the point of view of the pressure to be delivered, the flow rate to be delivered, the torque required of an electric motor, and other factors which are independent of machine vibration characteristics. Near the end of the design process, a vibration analysis is conducted on the rotor bearing system. If vibration problems are suggested by the analytical work, changes can be made in the rotor length or diameter, but this is relatively difficult since the designs are usually relatively fixed. Various bearing designs can be considered at this stage with the point of view of changing the rotor bearing critical speeds or reducing the rotor tendency toward instability. Currently, it is the design practice not to conduct a full rotor dynamics analysis considering critical speeds, unbalance response, and stability analysis for every machine which is produced. Thus, a machine may reach the test stand before a particular rotor dynamics problem is encountered. At this point, it is very difficult to redesign many aspects of the rotor besides the bearing. For these reasons, the designer and user of rotating machinery should be well acquainted with the fundamentals of vibration suppression characteristics on a number of different fluid film bearings.

A number of causes of large vibrations in rotating machinery exist. Machine unbalances normally produce large amplitudes of vibration which occur at the rotational frequency. Thus, this vibration is called a synchronous vibration because it is synchronous with the shaft speed. Machine instabilities due to hydrodynamic journal bearings themselves, interaction with the working fluid in a machine, seals in rotating machines, friction rubs, and internal friction due to stress reversals in shrunk on parts - all may produce vibrations which occur at a speed which is normally below that of the shaft rotational frequency. Thus, they are called subsynchronous vibrations. Additional machine vibrations may be caused by effects such as misalignment which normally creates a response at two times running speed (supersynchronous vibration pattern). Often, more than one cause of vibration occurs within a given operating machine so that the overall vibration pattern is quite complex. More than one change needs to be made in order to make the machine run with acceptable vibration characteristics.

It is important to have design information on optimum bearing configurations before entering into the design process. This is because there are so many geometrical choices for bearings that one cannot try all options in the

normal time frame. Also, a designer should have some idea as to how much machine stability can be increased by bearing changes. Stability increases are discussed both in this paper and in another by L. E. Barrett and E. J. Gunter elsewhere in this symposium. A critical question is "how well does current theory predict stability when compared to experiment?"

MULTILOBE BEARINGS

In this section some typical theoretical and experimental studies, which demonstrate the operating characteristics of multilobe bearings, are presented.

Linearized Stability Analysis for Multilobe Bearings

This section [1,2] investigates the problem of the linear stability and the nonlinear behavior of a single mass rigid rotor in four multilobe bearing configurations shown in Fig. 1: (a) an elliptical "lemon" shaped bearing (b) an offset elliptical bearing (c) a three-lobe bearing (d) a four-lobe bearing. All of the bearings have a length to diameter ratio of 0.5, preload factor and offset factor of 0.5 except the offset bearing for which the offset is 1.0. Stiffness and damping coefficients are given elsewhere and do not give much of a basis for comparing various bearing designs with one another. The linearized stability threshold is often used for this purpose. It should be emphasized that the linearized stability threshold assumes that the rotor is rigid, which is usually not correct. A full rotor stability analysis with both rotor and bearing properties must be conducted for any machine.

Since multilobe bearings do exhibit self-excited whirl vibration under certain speed and loading conditions, the designers are faced with the problem of selecting the bearing which will be the most stable or have the lowest force levels for a given application. Sometimes, bearings are classified as more stable simply because they are stiffer. A typical instability takes the form of half-frequency whirl occurring at shaft rotational speed of approximately two times the resonant frequency of a rotor system. The stiffer bearing is designated "more stable" because bearing stiffness increases the natural frequency which effectively raises the stability threshold speed at which bearing induced whirl will occur. In this study, all the bearings are oriented with the weight of the journal directly on the center of the bottom lobe. The ambient and cavitation pressures are taken to be zero. Film rupture is assumed to occur for negative pressures (the half Sommerfeld condition). The Reynolds equation is solved with the pressure at the leading and trailing edge of each bearing sector as well as on the sides assumed to be zero. The hydrodynamic pressure is integrated only over the region in which the pressure is positive.

The equations that lead to the determination of the bearing linearized stability for a rigid rotor are presented in [1]. Figure 2 shows the stability threshold speed ω_s plotted against Sommerfeld number for the four bearing types shown in Fig. 1. Each of the 45° straight lines with positive slope and constant η across the figures gives the locus of the operation of a bearing with a fixed geometry as it is brought up or down in speed. The bearing parameter η is defined as

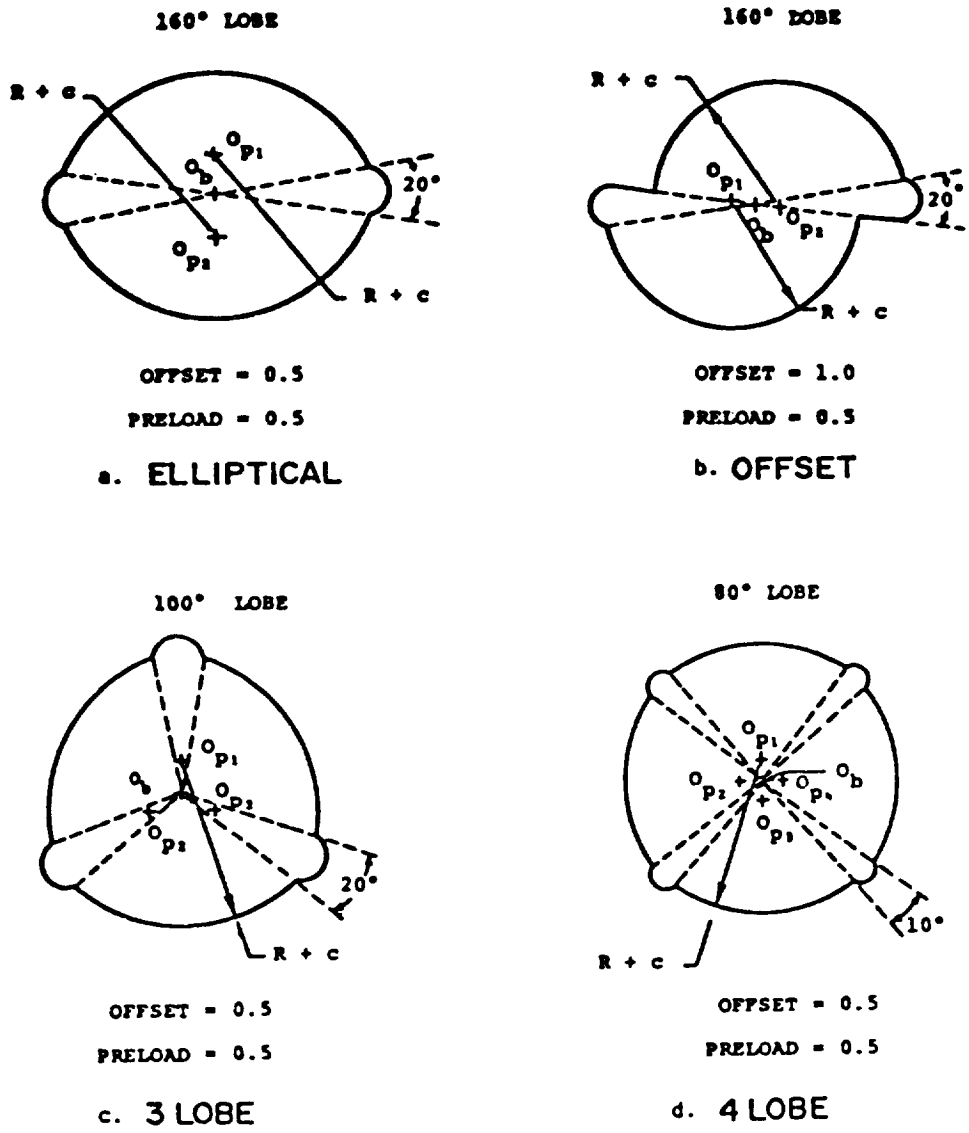

Figure 1 Multilobe Bearing Geometry

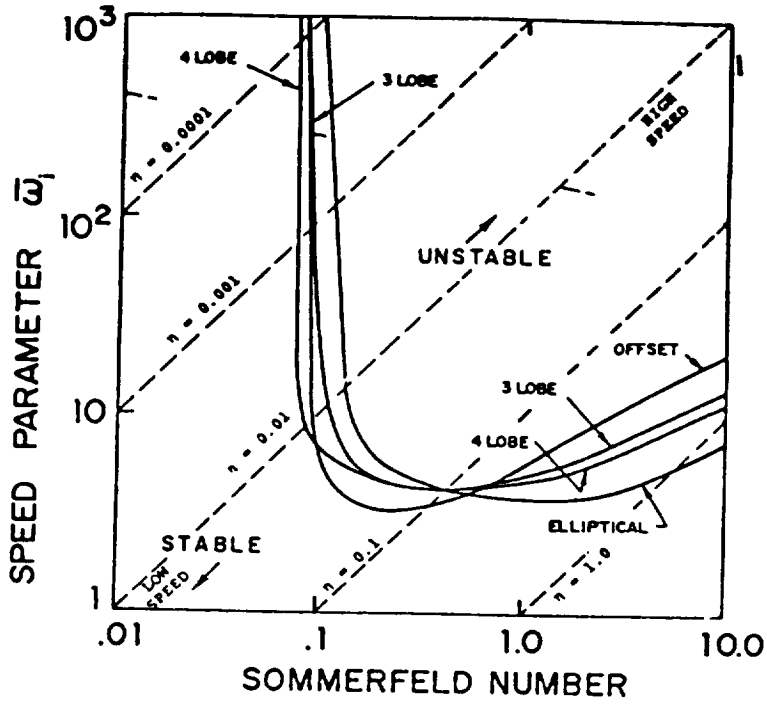

Figure 2 Linearized Bearing Stability for a Rigid Rotor

$$\eta = \frac{S}{\bar{\omega}_j} \frac{\mu LD}{8\pi W} \left(\frac{D}{c}\right)^2 \left(\frac{W}{cm}\right)^{1/2}$$

It should be noted that η is independent of the rotor speed and is in itself sufficient for the description of a certain bearing geometry on a stability graph. As a bearing increases in speed, it will proceed along a line of constant η and become unstable as it enters the unstable region by crossing the stability curve from below.

Figure 2 may be separated roughly into three regions: light load and/or close clearance (η = 0.1 to 1.0), moderate load and/or moderate clearance (η = 0.01 to 0.1) and heavy load and/or open clearance (η = 0.001 to 0.01). It is observed that under all operating conditions, the three-lobe bearing is consistently more stable than the four-lobe bearing except at η = 0.1 where the bearings have about the same stability threshold. All the other stability curves also appear to intersect roughly at this same point indicating little difference between the stability characteristics of the bearings in this area of operation.

At light load and/or close clearance operations, the offset bearing is the most stable. The three-lobe bearing is better than the four-lobe bearing by a small margin, while the elliptical "lemon" bearing is the least desirable. Within this region, the stability may be much improved by reducing the lobe clearance or effectively increasing the bearing parameter η.

Under moderate load conditions, the offset half bearing loses its superiority completely. The most stable bearing in this region is the elliptical bearings; followed by the three-lobe, the four-lobe, and the offset cylindrical bearing. Improvement in the stability performance by increasing lobe clearance or decreasing η is insubstantial on the high η side within this regior

At heavy load and/or open clearance operations, the order of increasing stability is: the four-lobe bearing, the offset bearing, the three-lobe bearings, and the elliptical bearing. Increasing lobe clearance or decreasing η will drastically improve the stability threshold for all of the bearings.

While the offset bearing is superior in stability for light load operation, the elliptical bearing appears to be most stable for a wide range from heavy loaded to relatively lightly loaded applications.

Although the three-lobe bearing does not have the best stability, it offers good overall performance under all load conditions. It is second only to the most stable bearing in each region.

Using a single mass flexible rotor, it can be shown that the flexible rotor stability threshold is given by [1]

$$\bar{\bar{\omega}}_s = \frac{\bar{\omega}_s}{\left[1 + \bar{\omega}_s^2 \, \bar{\omega}_d^2 \left(\frac{g}{c\omega_r^2}\right)^2\right]^{1/2}}$$

where ω_r is the rotor critical speed on rigid bearings. Because the stability threshold for a flexible rotor is always lower than that for a rigid rotor, Fig. 2 should be viewed as the highest possible stability that can be achieved in these bearings.

One of the major concerns in this investigation is the stability of the multi-lobe bearings in light load applications. The non-linear characteristic of the bearings examined in this section are to have the bearing parameter η = 0.3. Insofar as possible, generalization of the results throughout this paper is provided by the use of dimensionless parameters instead of particular bearing specifications and operating conditions. An example bearing with η = 0.3 is

L = 38.1 mm (1.5 in.)
D = 76.2 mm (3.0 in.)
c = 0.152 mm (0.006 in.)
W = 168.3 N (37.8 lb)
$\mu = 6.89 \times 10^{-3}$ N-s/m^2 (1.0×10^{-6} lb-s/in.^{2})

For comparison to the transient analysis, the linear stability thresholds, corresponding Sommerfeld numbers, and whirl speed ratios for the four bearing types at η = 0.3 are tabulated in Table 1. The journal speeds for each of the four bearing types are at the threshold speeds of instability are also shown. The order of increasing stability is: the elliptical bearing, the four-lobe bearing, the three-lobe bearing and the offset bearing.

Bearing Type	Sommerfeld Number S	Whirl Ratio $\bar{\omega}_d$	Stability Threshold $\bar{\omega}_s$	Bearing ω_s (RPM)
Elliptical	1.15	.495	3.82	9,252
4-Lobe	1.52	.475	5.08	12,304
3-Lobe	1.86	.470	6.21	15,041
Offset	3.62	.361	12.07	29,234

Table 1 Stability Thresholds and Whirl Ratios for Various Bearing Types with Bearing Parameter $\eta = 0.3$

Four Lobe Bearings in a Single Mass Flexible Rotor

In this section, a flexible rotor was mounted in a set of four-lobe bearings. Dynamic behavior and the instability threshold was investigated for several configurations (for more details see Ref. [3]). All parameters were held constant for all tests with the exception of the value of the load angle θ_g. For a four lobe bearing $\theta_s = \gamma_g$. Small changes in this parameter were seen to change the dynamic response considerably. The specifications of the two bearings are summarized in Table 2. The same two bearings were used for all of the tests in this section.

	Bearing 1	Bearing 2
Shaft Diameter D (mm) $\pm$ 0.003	25.377	25.342
Radial Clearance, c_r (mm) $\pm$ 0.003	0.041	0.058
Lobe Clearance, c_ℓ (mm) $\pm$ 0.003	0.178	0.193
Preload Factor, m $\pm$ .025	0.77	0.70
Pad Angle, χ	63°	63°
Bearing Length, L (mm) $\pm$ .05	14.22	14.22
L/D Ratio $\pm$ .003	0.559	0.559
Offset Factor, α	0.50	0.50

Table 2 Four-Lobe Bearing Specifications

The first orientation to be discussed is $\theta_g = -15°$. Figure 3 shows the synchronous motion, total motion, and phase angle responses for rotor run-up for the X2 probe. In this figure, the two most important features are the responses at the rotor first critical speed and at high speeds. First, the rotor is seen to remain stable for all speeds. The maximum speed that the rotor was run at approximately 12,500 RPM and neither the total nor synchronous motion of the rotor displayed any large limit cycle vibration. The overall motion did, however, gradually tend to increase as the speed increased above 6000 RPM. Second, the motion of the rotor at the critical speed is seen to increase.

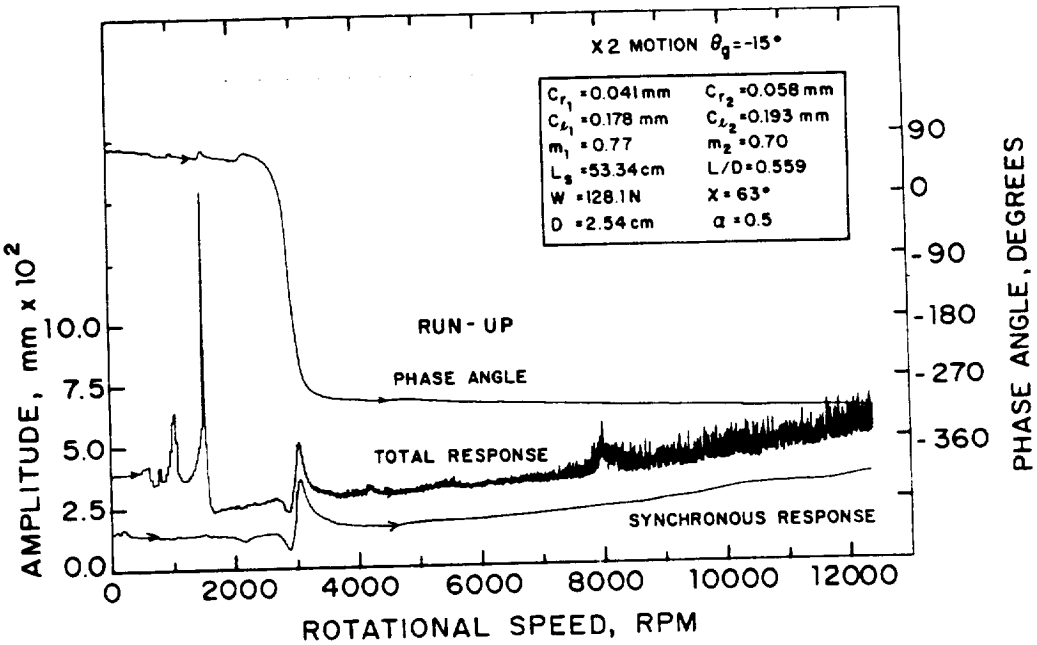

Figure 3 Total and Synchronous X2 Motion (Run-up) for $\theta g = -15°$

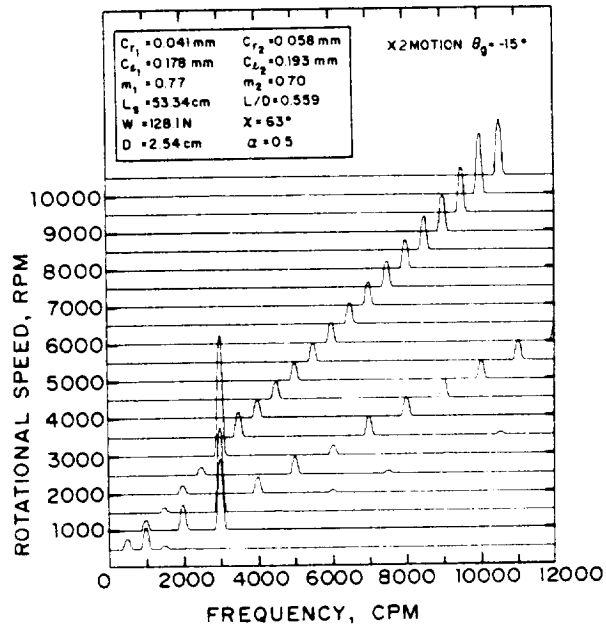

Figure 4 Waterfall Frequency Spectrum X2 Motion for $\theta g = -15°$

The waterfall frequency spectrums are presented for the X2 motion in Fig. 4. Such a figure complements the synchronous response plots well. For example, the supersynchronous excitation of the rotor critical speed can easily be seen. Also, the 2x and 3x components that contribute to the total observed motion can easily be seen. Lastly, no subsynchronous motion was seen at any time in the operation range. This rotor-bearing system was thus very stable throughout this test.

The second configuration discussed is $\theta_g = 30°$. The X2 total and synchronous motion and phase angle responses are presented for rotor run-up in Fig. 5. The rotor went unstable very rapidly at 6600 RPM, as indicated by the total motion. Thus, rotating the bearings 45° from the initial position reduced the stability threshold by more than 5900 RPM. On run-down the rotor was locked in an unstable condition has also been observed for pressure dam bearings but has not been observed for axial groove bearings with no preload.

The waterfall frequency spectrum for $\theta_g = 30°$ (X2 motion, run-up) is presented in Fig. 6. This figure is presented to demonstrate the frequency at which the rotor was vibrating during the unstable condition. This frequency is the same as the critical speed of the rotor (approximately 3000 CPM). Other configurations which became unstable also oscillated at this same frequency and the rotor was never seen to demonstrate any half frequency oil whirl. Thus, when this rotor-bearing system demonstrated any instabilities, the condition was whip as opposed to whirl.

Using the results presented above and the results from other tests, the instability threshold speed was correlated with the angular position of the groove (θ_g). This plot is presented in Fig. 7. Also plotted in Fig. 7 is the end of the hysteretic effect of whip run-down. As can be seen from this figure, the optimum location of the grooves is for a value of θ_g from -15° to 0°, or from 75° to 90°. The worst case is when $\theta_g = 30°$. On the other hand, the end of whip on run-down is not seen to be a strong function of θ_g. This level remained between 5800 RPM and 7400 RPM for all cases when the system went unstable. This implies that the higher the rotor instability threshold, the longer the rotor will demonstrate whip during run-down. This observation was also made for pressure dam bearings.

The experimental data is next correlated with theoretical predictions. For this section, finite elements were utilized to calculate the bearing coefficients for the four-lobe bearings used here. Also, the flexible rotor was modeled using lumped rotor masses [4]. This model was then used with the bearing coefficients to predict the stability of the rotor-bearing system. This stability threshold was calculated for various values of θ_g and the theoretical predictions are presented in Fig. 7. As can be seen, significant differences exist between the experimental data and theoretical predictions for the instability threshold ranging from 400 RPM at $\theta_g = 30°$ to over 4900 RPM at $\theta_g = 0°$. Two reasons may account for these discrepancies. First, the theoretical method, which was used, was based on the half-Sommerfeld boundary condition with isoviscous theory. Using the Reynolds boundary condition and the effect of viscosity in the solution of the differential equations is probably more realistic. Second, small inaccuracies in the dimensions of the shaft and bearings will certainly affect the rotor-bearing stability. Nonetheless, the experimental and theoretical results are in

semi-quantitative agreement since the optimum value of θ_g is the same for both (θ_g = -15° or 75°). This value of γ_g (or θ_g for this case) is the same as for the three lobe bearings in a rigid rotor.

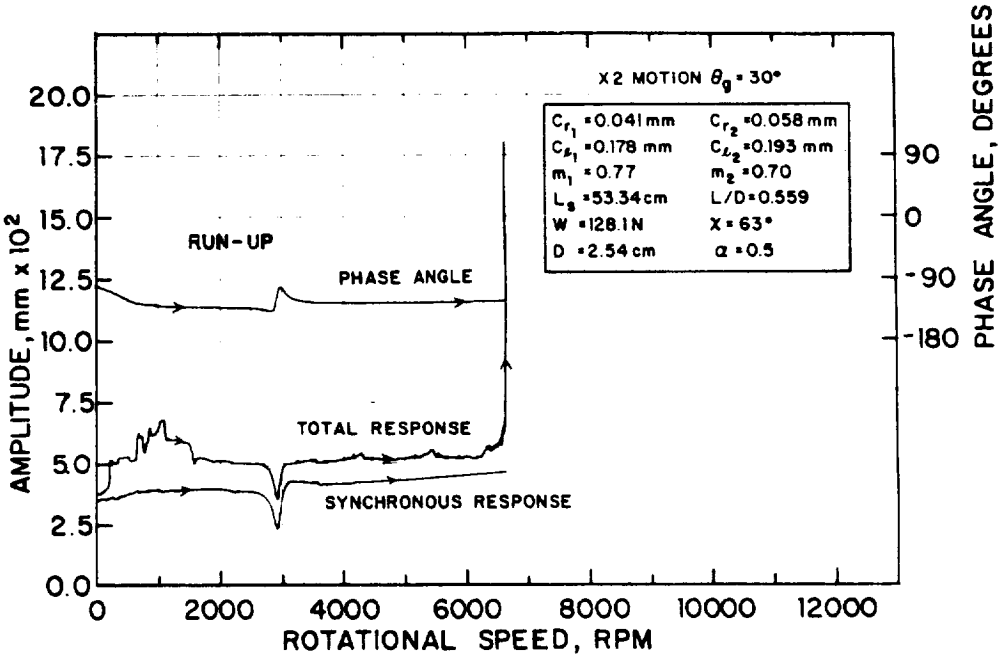

Figure 5 Total and Synchronous X2 Motion (Run-up) for θ_g = 30°

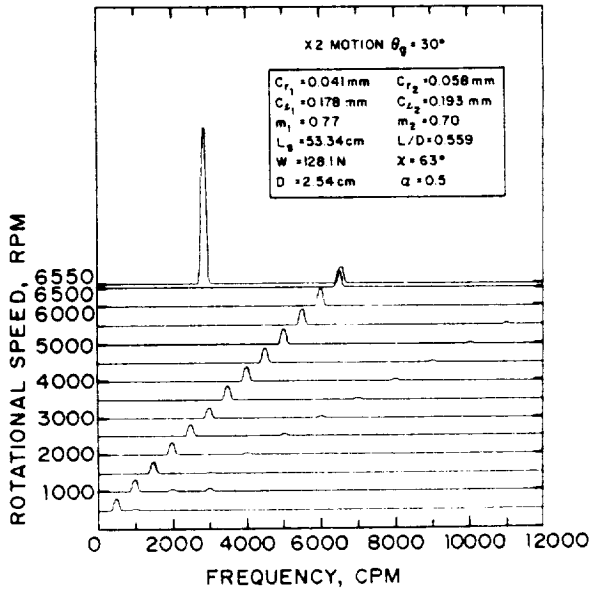

Figure 6 Waterfall Frequency Spectrum for X2 Motion for θ_g = 30°

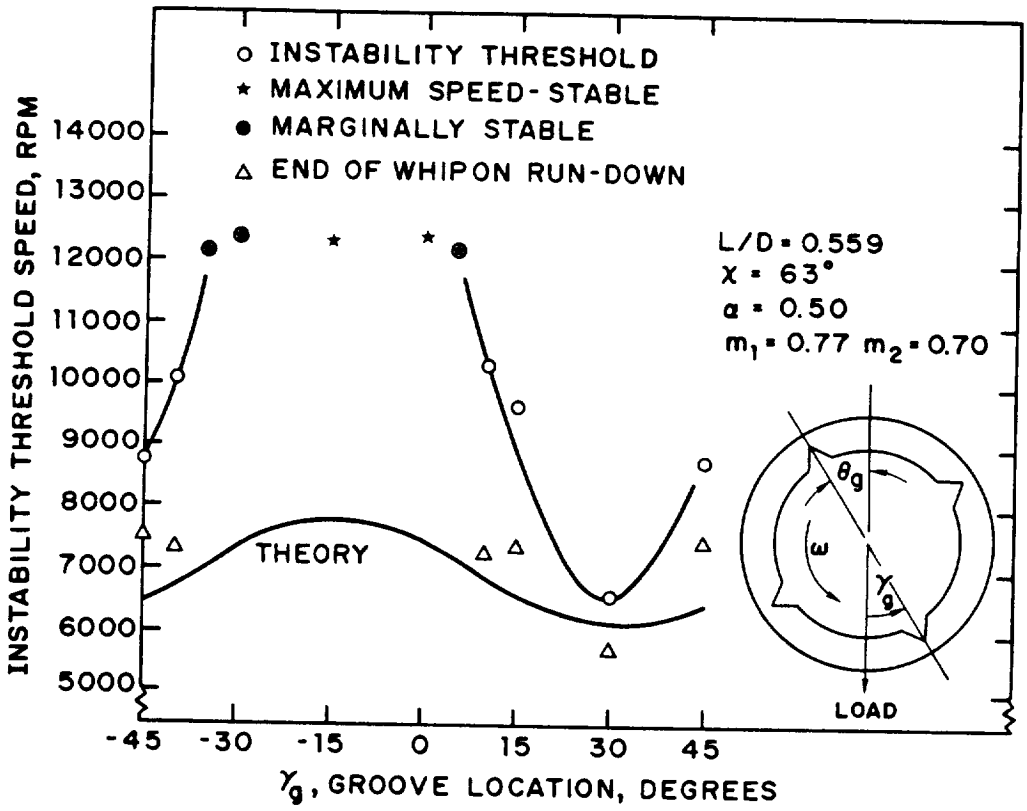

Figure 7 Summary of Correlation of Instability Threshold Speed with γ_g

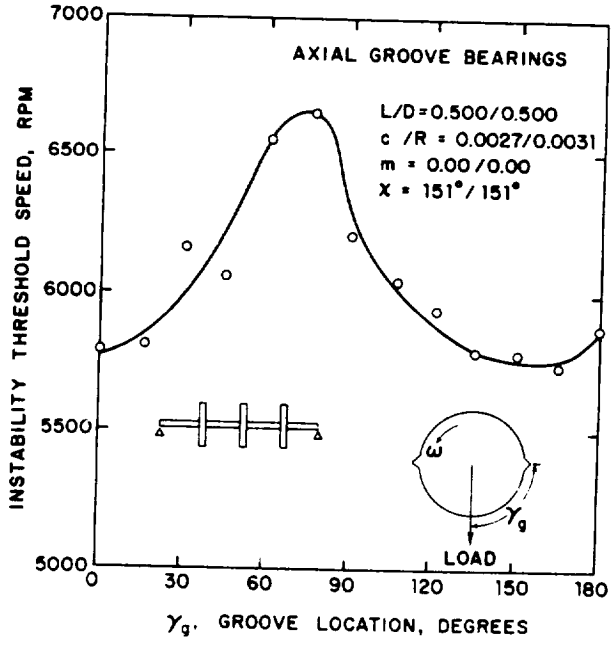

Figure 8 Summary of Correlation of Instability Threshold Speed with γ_g

2 Axial Groove Bearings in a 3 Mass Flexible Rotor

Axial groove bearings have been tested in a 3 mass flexible rotor in a similar manner to the studies done in the previous subsection. The apparatus is similar to the single mass flexible rotor. The specifications of the bearings are presented in Table 3. For brevity only, the summary graph is presente here (Fig. 8). As can be seen, the instability threshold is considerably lower for these bearings than for the four lobe bearings in the single mass rotor. There are two reasons for this. First and most importantly, the preload for these bearings is zero. Second, this apparatus is more flexible due to the smaller shaft diameter. The instability threshold does vary with the load angle and the optimum value of γ_g is once again approximately 75°.

Table 3 Two Axial Groove Bearings

	Bearing 1	Bearing 2
Shaft Diameter, D (mm)	25.397	25.387
Clearance, c (mm)	0.037	0.042
Pad Angle, χ	151°	151°
Length, L (mm)	12.70	12.70
Preload, m	0.00	0.00

PRESSURE DAM BEARINGS

Linearized Stability Analysis for Step Bearings

Pressure dam or step journal bearings have long been used to improve the stability of rotating machinery. They can replace plain journal or axial groove bearings in machines operating at high speeds and increase the stability threshold. A step or dam is cut in the upper half surface of the bearing producing a pressure rise near the step and a hydrodynamic load on the journal.

At high speeds and/or light loads, the step creates a loading that maintain a minimum operating eccentricity. That is, as speed is increased, the bearing eccentricity does not approach zero as it would for plain journal or two axial groove bearings. The eccentricity approaches some minimum value or may even increase with increasing speed due to the step loading. Thus, a properly designed step bearing would operate at a moderate eccentricity even at high Sommerfeld numbers [5,6].

Consider a finite length step bearing as shown in Figs. 9 and 10. Many industrial bearings have two oil supply grooves in the horizontal plane and a step located in the second quadrant with counterclockwise shaft rotation. A rectangular dam is usually used. A circumferential relief groove or track is sometimes grooved in the bottom half of the bearing. Both of these effects (dam and relief track) combine to increase the operating eccentricity of the bearing when compared to a plain journal or two axial groove bearing.

Many geometric variables affect the performance of pressure dam bearings. For all of the step journal bearings analysis in this paper, two 20° oil inlet grooves are located at θ = 0° and θ = 180°. Also, the dam axial length ratio

is held constant at $\bar{L}_d = 0.75$ for all cases. To study the effects of the remaining variables, only one is changed while the others remain the same. The base line design is

$L/D = 1.0$
$Re_2 = 210$

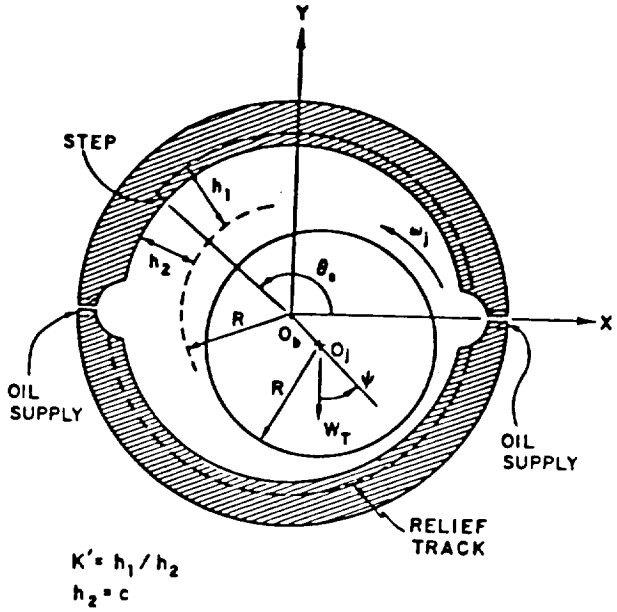

Figure 9 Pressure Dam Bearing Schematic, Side View

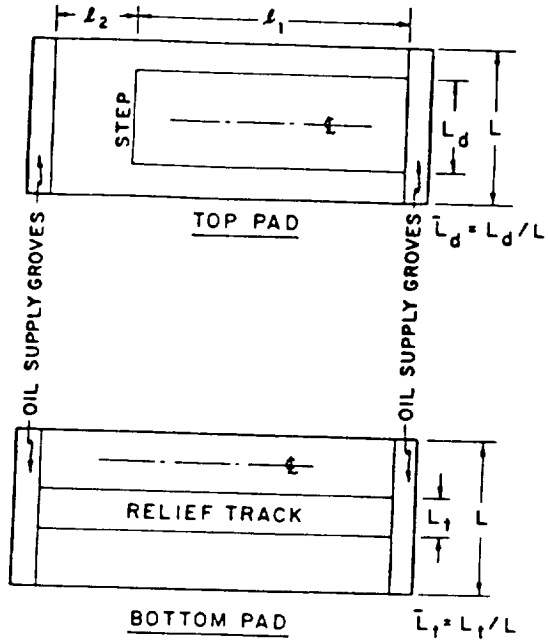

Figure 10 Pressure Dam Bearing Schematic, Top and Bottom Pads

$\theta_s = 125°$
$K' = 3.0$
$\bar{L}_t = 0.25$

This section analyzes the finite pressure dam bearing neglecting step inertia effects, but including the effects of turbulence over the entire bearing surface. Bearing stability threshold curves for vairous pressure dam bearing geometries are compared to plain journal, two axial groove and grooved lower half bearings. The effects on stability threshold of film thickness ratio, dam location, and other geometric parameters are considered. Optimum bearing designs are suggested to provide favorable stability characteristics.

Figure 11 compares the stability characteristics of the plain journal, two axial groove and grooved lower half bearings to two types of pressure dam bearings. The stability threshold speed ω_s is plotted against the Sommerfeld number, S. Also indicated at the top is the bearing eccentricity ratio ε_b for all five bearings. Bearing numbers 1 and 2 are the plain journal and two axial groove bearings, respectively. Note that at high Sommerfeld numbers the stability curves for each approach asymptotic values of $\omega_s = 2.3$ (plain journal) and $\omega_s = 2.05$ (2 axial groove).

Bearing number 3 is the grooved lower half bearing. This bearing is simply a two axial groove bearing with a circumferential relief track or groove cut in the lower half. In this case, the relief track axial length ratio (see Fig. 18) is $\bar{L}_t = 0.25$ (the relief track is 25% of the bottom pad). A considerable increase in the infinite stability region is evident. That is, the plain journal bearing is theoretically stable at all speeds below a Sommerfeld number of 0.48, while the grooved lower half bearing increases this range of infinite stability by a factor of 3 to $S \leq 0.17$. The relief track removes part of the bearing load carrying surface for the bottom pad thereby allowing bearing number 3 to reach 0.8 eccentricity at a higher Sommerfeld number than the plain journal bearing. Around $\varepsilon_b = 0.8$, $\bar{K}_{xy}$ changes sign providing the favorable stability characteristics. Essentially no increase in stability is seen at high Sommerfeld numbers.

Bearing number 4 is a pressure dam bearing with $K' = 3.0$ (dam clearance 3 times as large as the bearing clearance) and $\bar{L}_t = 0.0$ (no relief track). For this case, the stability is increased compared to the journal bearing at high Sommerfeld numbers while the region of infinite stability is less. As discussed earlier, at high Sommerfeld numbers the step forces the journal to operate at a moderate eccentricity. From the top of Fig. 21, bearing number 4 operates at an eccentricity ratio of $\varepsilon_b = .25$ at $S = 5.5$. This moderate eccentricity provides the favorable stability characteristics at high Sommerfeld numbers for this step journal bearing.

Combining the two effects of a relief groove in the lower half and a step in the upper half, bearing number 5 is a dam bearing with $K' = 3.0$ and $\bar{L}_t = 0.25$. For this case, the stability is increased for the entire range of Sommerfeld numbers compared to the journal bearing. The two separate effects of a pressure dam bearing are shown clearly in Fig. 21. The relief track forces the bearing to operate at higher eccentricities thereby increasing the region of

infinite stability. The dam loads up the journal at high Sommerfeld numbers providing a moderate operating eccentricity and higher stability threshold.

The effect of varying the film thickness ratio K' on stability was carried out but is not shown here. Reference [6] concludes that the optimum (as far as load capacity is concerned) is approximately $K' = 3.0$. A bearing with a film thickness ratio of $K' = 6.0$ is only slightly less superior (a 10% decrease at $S = 10.0$). A 40% decrease in stability is evident for a step bearing with $K' = 12.0$ when compared to the $K' = 3.0$ bearings at $S = 10.0$.

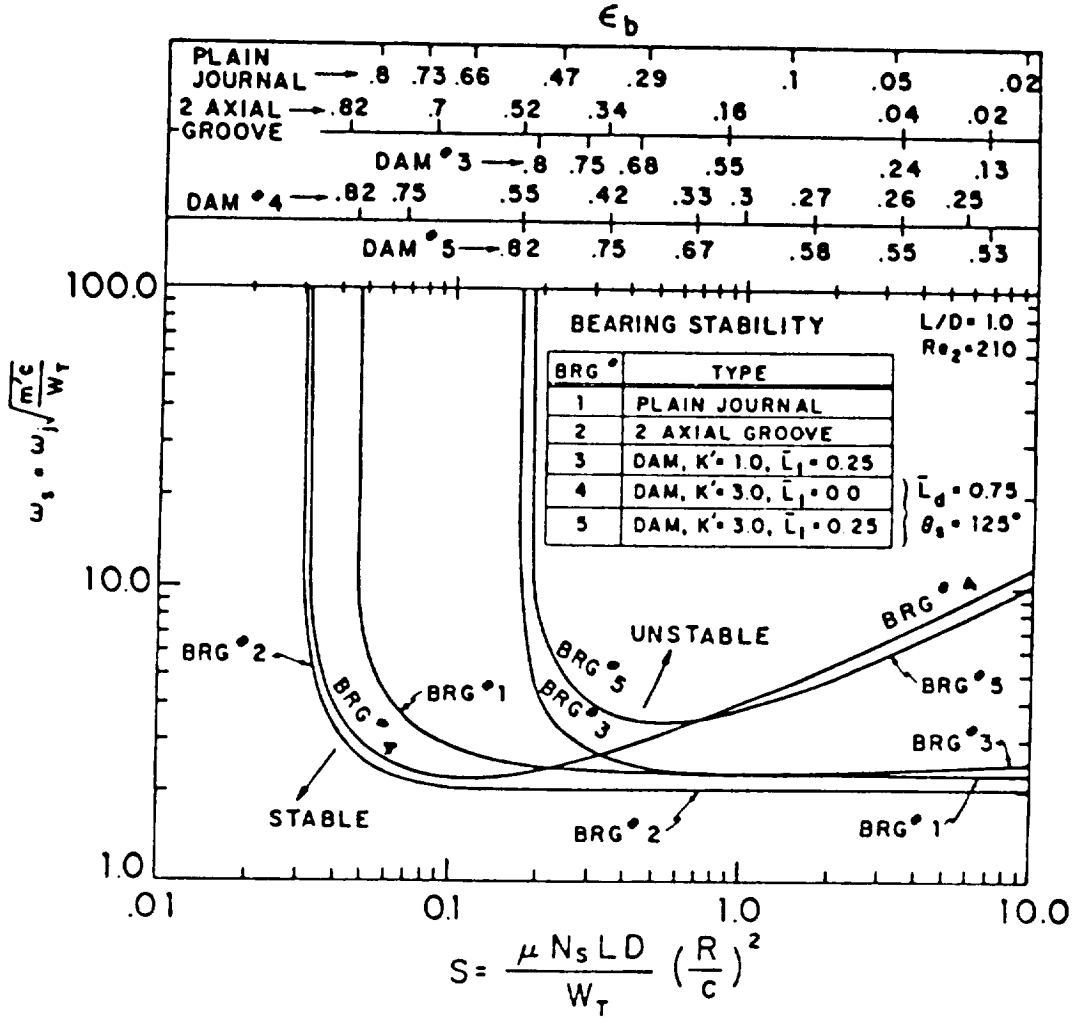

Figure 11 Stability Map Comparing Pressure Dam Bearings to Plain Journal and Two Axial Groove Bearings

The important geometric parameters in pressure dam bearing design are the film thickness ratio, K' and the dam location, θ_s. Steps should be located at around $\theta_s = 145°$ or 150°, while K' values of between 3.0 and 6.0 are recommended.

From Sommerfeld numbers above S = 2.0, step journal bearings designated with near optimum step location and size can increase the rigid rotor stability parameter ω_s by a factor of 10 or more over a plain journal bearing. Additionally, the pressure dam bearing would operate at a moderate eccentricity ratio (between $\varepsilon_b = 0.25$ and $\varepsilon_b = 0.5$) even though the loading is light and/or speed high. However, for Sommerfeld numbers below S = 2.0, a step bearing will increase ω_s only slightly (by a factor of around 1.5) over a plain journal bearing even if the optimum dam height and location were used.

Experimental Step Bearing Stability in a Single Mass Flexible Rotor

Experimental results are given for different step configurations in the same experimental flexible rotor described in [7]. A theoretical-experimental comparison of the instability onset speed for the simple flexible rotor is presented [7,8]. Five different step bearing geometries and a two axial groove bearing are considered. The pressure dam bearings employed have different step heights and locations. Optimum and off-optimum designs are used. Instability onset speeds are determined both theoretically and experimentally and a comparison is made to determine the accuracy of the theoretical analysis.

All six pairs of bearings considered have two axial oil supply grooves located at the horizontal split (Fig. 9). These grooves are 20° in arc length making the arc length of both top and bottom pads 160°. The step bearings do not contain a circumferential relief groove in the bottom pad. The two axial groove bearings are identical to the pressure dam design with $h_1 = h_2$ in Fig. 9. The length to diameter ratio for each bearing is 1.0 with D = 2.54 cm.

Ideally, each bearing was to have a 5.08×10^{-3} cm (2.0 mil) radial clearance. However, due to difficulties in manufacturing, the radial clearance ranged from 4.57×10^{-3} to 6.35×10^{-3} cm (1.8 to 2.5 mils). The clearance was measured cold with a dial micrometer. Several readings were taken and the aver age value used.

The important geometric parameters in step bearing design are the film thickness ratio K' and the dam location θ_s. The ratio of film thicknesses is defined as h_1/h_2 when the shaft is centered in the bearing (Fig. 10). Thus, $K' = h/h$, $K'^1 = h_1/c$ where h_1 = centered clearance inside pocket. The dam location angle θ_s is measured with rotating from the positive x (horizontal) axis. Optimum values for favorable stability are around $K' = 3.0$ and $\theta_s = 125°$ to 150°. Other parameters are the dam axial length ratio $\bar{L}_d = L_d/L$ (Fig. 3) and the reliev groove axial length ratio $\bar{L}_t = L_t/L$. For all cases, $L_t = 0.0$, since the bottom pad does not have a circumferential relief groove.

A summary of these parameters is listed in Table 4 for all six sets of bearings. Note that step bearing sets 1 and 2 represent the near optimum design with film thickness ratios between 2.1 and 2.8. Sets 3 and 5 are off-

optimum designs with larger K′ values between 6.6 and 11.7. The off-optimum angular location is represented by set 4 with $\theta_s = 90°$. The dual numbers in the Table refer to the left (motor) and right ends of the test rotor, respectively.

Bearing Set No.	Type	K′	θ_s	c (cm x 10^3)	c (mils)	$\bar{L}_d$
A	Two Axial Groove	1.0 1.0	- -	4.57 5.08	1.8 2.0	- -
1	Step	2.1 2.4	145°	5.59 6.35	2.2 2.5	0.75
2	Step	2.8 2.6	140°	6.35 6.35	2.5 2.5	0.75
3	Step	6.6 8.6	150°	6.10 6.35	2.4 2.5	0.75
4	Step	3.3 2.1	90°	6.10 6.10	2.4 2.4	0.75
5	Step	11.7 8.3	140°	5.33 6.10	2.1 2.4	0.50

Common to all bearings: $L/D = 1.0$, $\bar{L}_t = 0.0$, $\chi = 160°$

Table 4 Summary of Geometric Parameters for the Six Bearing Sets

Table 5 summarizes the experimental results. The near-optimum designs (sets 1 and 2) increase the instability onset speed by 109 and 41 percent, respectively, over the two axial groove bearings. The off-optimum designs (sets 3, 4, and 5) increase the instability speed by 35, 30, and 18 percent, respectively.

Comparing step bearing set number 3 to number5, increasing the film thickness ratios from 6.6 and 8.6 to 11.7 and 8.3 decreases the instability speed by 12 percent. This trend is somewhat tainted since the dam axial length ratio is smaller for set 5 compared to set 3. Also, the step locations differ by 10°.

To obtain the theoretical instability onset speeds, the stiffness and damping properties of the bearings must be determined. The dynamic properties for all six sets of bearings were calculated using a finite element step bearing computer program that solves the Reynolds equation using finite elements [6]. The speed dependent characteristics are used as input data to a stability program that employs a transfer matrix approach similar to the method presented in Ref. [4].

Bearing Set No.	Type	K′	θ_s	Instability Onset Speed (RPM)		Percent Error
				Theoretical	Experimental	
A	Two Axial Groove	1.0	-	6,000	6,600	9.1%
1	Step	2.1, 2.4	145°	11,100	>13,800	>19.6%
2	Step	2.8, 2.6	140°	11,500	9,300	-23.7%
3*	Step	6.6, 8.6*	150°	8,850	8,900	0.6%
4*	Step	3.3, 2.1	90°*	8,100	8,600	5.8%
5*	Step	11.7, 8.3*	140°	7,800	7,800	0.0%

* Off-optimum

Table 5 Summary of Theoretical Instability Onset Speeds for the Six Bearing Designs

Table 5 summarizes the results of the theoretical stability analysis. The experimental results are also indicated along with the percent error in the theoretical predictions. The error is under 10 percent for all cases except step bearing sets 1 and 2. Set number 1 has an error greater than 19.6 percent Set number 2 overestimates the onset speed by 23.7 percent. All other cases theoretically underpredict the instability speed.

The near-optimum pressure dam bearing designs increase the instability onset speed of the single mass rotor by around 109 and 41 percent compared to the two axial groove bearings. Increasing the film thickness ratio from the near-optimum cases decreases the onset speed. Decreasing the step location to 90° from the near-optimum locations also decreases the onset speed.

Pressures have also been measured in step bearings [9] and compared to theoretical predictions. Pressure measurements qualitatively agree with the stability measurements. Namely, sets 1 and 2 produce the largest pressures at the steps, which result in large artifical loads and good stabilizing charac teristics.

The theoretical stability analysis predicts the general trends in the experimental data. All step bearing designs increase the onset speed over the two axial groove bearings. The near-optimum designs have the highest onset speeds and the off-optimum designs the lowest.

Side rail construction is important in designing step bearings for optimum stability. Care should be taken to insure uniform pocket depth.

In many field applications, if a rotor system is unstable with simple axial groove bearings, one of the common "fixes" is to simply mill a step in the upper half of the bearing. Present results indicate that such a procedure will not guarantee machine stability, even for optimum values of K'.

CONCLUSIONS

Two types of fixed pad hydrodynamic bearings - multilobe and pressure dam - have been considered here. Optimum and non-optimum geometric configurations were tested. The optimum geometric configurations were determined by using a theoretical analysis and then the bearings were constructed for a flexible rotor test rig. It has been found that optimizing bearings using this technique can produce a 100% or greater increase in rotor stability. It should be noted that this increase in rotor stability was carried out in the absence of certain types of instability mechanisms such as aerodynamic cross-coupling. However, the increase in rotor stability should greatly improve rotating machinery performance in the presence of such forces as well. More work remains to be done in this area.

Very significant differences between the experimentally observed stability threshold for certain bearings and the theoretically predicted stability thresholds have been observed. The theoretical results using an isoviscous standard solution of Reynolds equation predicts an increase of something like 10-40% in the stability threshold. There was, therefore, little reason to suspect that optimization of the bearing design would be very worthwhile to investigate. However, when the bearings were constructed and put in the experimental rig, the increase in stability was often greater than a 100% increase. Thus, the optimum bearing designs would appear to be much more worthwhile investigating than previously suspected.

It is also interesting to note that the experimental result was better than the theoretical prediction in all cases. While only a few of the experimental results actually carried out are presented in this paper, a number of other results not directly reported here show the same tendencies. The higher experimental stability threshold was true for various bearing types, bearing manufacturers, distribution of mass on the shaft, type of oil used to lubricate the bearings, bearing surface type, and a number of other factors. Experimentally observed pressures taken for one bearing type were also significantly higher than the peak pressures predicted by theory.

It is apparent from our research that some of the current theories normally used for bearing designs and rotating machinery may not be adequate. It appears that for bearings where a strongly converging area exists in the bearing, such as in both the multilobe and pressure dam pressures considered in this case, a more careful job must be done on the theoretical analysis. Some increases in stability threshold due to the use of Reynolds boundary conditions, temperature effects in the fluid, and other effects may increase the theoretical stability threshold somewhat. Results available to these authors indicate that these increases are not sufficient to give good agreement to theory and experiment. It appears likely that some detailed pressure measurements should be made for beaings involving a film thickness change of 3 to 6 times over one pad length

as shown by the optimum cases in this work.

Several possible effects could be occurring in these bearings. Turbulence theories may not be adequate although some of these effects have been investigated by the authors and found to be small for these bearings. Other theories which may prove worthwhile to investigate could include visco-elastic effects for the rapid changes in the film thickness. Perhaps some combination of all of the above effects would produce a much better agreement between theory and experiment.

It can be seen from the results in this paper that one cannot yet say that the optimum designs for journal bearings are well known. Based on the experimental results one cannot even say that one knows accurately the upper limit for stability produced by journal bearings of various types. The effect that all of this has in the presence of other forces is yet to be known. One major encouraging factor is that when one looks at an optimum bearing design using the current theoretical analysis, one does always predict the best bearing for the situation involved. One may also expect that in most cases it will perform better than theory would tell one.

ACKNOWLEDGEMENTS

The work described in this paper has largely been published elsewhere as indicated in the References. This paper is intended as a sampler of different works carried out for several bearing types in order to provide an introduction to bearing design for the user of turbomachinery.

Various phases of the work reported in this paper have been supported in part by U.S. Department of Energy Contract No. DE-ACo1-79ET-13151, NASA Lewis Research Contract No. NSG-3177-1, Engineering Foundation Grant No. RC-A-77-6C, and the University of Virginia Industrially Supported Program for the Dynamic Analysis of Turbomachinery under the direction of Dr. Edgar J. Gunter.

REFERENCES

1. Allaire, P. E., "Design of Journal Bearings for High Speed Rotating Machinery," in Fundamentals of the Design of Fluid Film Bearings, ASME Publication, 1979, pp. 45-84.

2. Li, D. F., Choy, K. C., and Allaire, P. E., "Stability and Transient Characteristics of Four Multilobe Journal Bearing Configurations," accepted for

publication in Journal of Lubrication Technology, Trans. ASME, Paper No. 79-Lub-3.

3. Leader, M. E., Flack, R. D., and Lewis, D. W., "An Experimental Determination of the Instability of a Flexible Rotor in Four-Lobe Bearings," Wear, Vol. 58, No. 1, 1980, pp. 35-47.

4. Lund, J. W., "Stability and Damped Critical Speeds of a Flexible Rotor in Fluid-Film Bearings," Journal of Engineering for Industry, Trans. ASME, Vol. 96, No. 2, May 1974, pp. 509-517.

5. Allaire, P. E., Nicholas, J. C., and Barrett, L. E., "Analysis of Step Journal Bearings - Infinite Length, Inertia Effects," Trans. ASLE, Vol. 22, No. 4, October, 1979, pp. 333-341.

6. Nicholas, J. C. and Allaire, P. E., "Analysis of Step Journal Bearings - Finite Length, Stability," to be published in ASLE Trans., No. 78-LC-6B-2.

7. Leader, M. E., Flack, R. D., and Allaire, P. E, "The Experimental Dynamic Response of a Single Mass Flexible Rotor with Three Different Journal Bearings," accepted for publication in ASLE Trans. Preprint No. 79-AM-6D-2.

8. Nicholas, J. C., Barrett, L. E., and Leader, M. E., "Experimental-Theoretical Comparison of Instability Onset Speeds for a Three Mass Rotor Supported by Step Journal Bearings," accepted for publication in ASME Trans., Journal of Mechanical Design, Preprint No. 79-DET-56.

9. Flack, R. D., Leader, M. E., and Allaire, P. E., "Experimental and Theoretical Pressures in Step Journal Bearings," accepted for publication in ASLE Trans.

APPENDIX

Bearing Summary Charts

Table 6 gives some of the advantages and disadvantages of various bearing types in condensed form. The bearing stability or resistance to whirl has been explored in some depth in the earlier sections. Other comments such as "good damping at critical speeds" have come from the authors' experience. The table represents input from many different sources.

In summary, a wide range of bearing designs are available to the designers and users of rotating machinery. These range from very simple plain journal bearings, which are low in cost and easy to make, up to very complex tilting pad bearings which have many components and require very careful design. These can be used to reduce or eliminate vibration problems in many rotating machines. The cost and ease of manufacture must be balanced with the requirements for suppression of non-synchronous vibration in rotating machines.

Table 6a Fixed Pad Non-Preloaded Journal Bearings

Bearing Type	Advantages	Disadvantages	Comments
Plain Journal	1. Easy to make 2. Low cost	1. Very subject to oil whirl	Round bearings are nearly always "crushed" to make elliptical bearings
Partial Arc	1. Easy to make 2. Low cost 3. Low horsepower loss	1. Poor vibration resistance 2. Oil supply not easily contained	Bearing used only on rather old machines
Axial Groove	1. Easy to make 2. Low cost	1. Subject to oil whirl	Round bearings are nearly always "crushed" to make elliptical or multi-lobe
Floating Bush	1. Relatively easy to make 2. Low cost	1. Subject to oil whirl	Used primarily in high speed turbo-chargers for diesel engines in trucks and buses

Table 6b Fixed Pad Preloaded Journal Bearings

Bearing Type	Advantages	Disadvantages	Comments
Elliptical	1. Easy to make 2. Low cost 3. Good damping at critical speeds	1. Subject to oil whirl at high speeds 2. Load direction must be known	Probably most widely used bearing at low or moderate speeds
Offset Half (With Horizontal Split)	1. Excellent suppression of whirl at high speeds 2. Low cost 3. Easy to make	1. Fair suppression of whirl at moderate speeds 2. Load direction must be known	Has high horizontal stiffness and low vertical stiffness-may become popular-used outside U.S.
Three and Four Lobe	1. Good suppression of whirl 2. Overall good performance 3. Moderate cost	1. Some types can be expensive to make properly 2. Subject to whirl at high speeds 3. Goes unstable with little warning 4. Very high vibration levels during instability	Currently used by some manufacturers as standard bearing design

Table 6c Fixed Pad Journal Bearings with Steps, Dams or Pockets

Bearing Type	Advantages	Disadvantages	Comments
Pressure Dam (Single Dam)	1. Good suppression of whirl 2. Low cost 3. Good damping at critical speeds 4. Easy to make	1. Goes unstable with little warning 2. Dam may be subject to wear or build-up over time 3. Load direction must be known 4. Does not suppress whirl for very flexible rotors	Very popular with petro-chemical industry. Easy to convert elliptical over to pressure dam
Multi Dam Axial Groove or Multilobe	1. Dams are relatively easy to place in existing bearings 2. Good suppression of whirl 3. Relatively low cost 4. Good overall performance	1. Complex bearing requiring detailed analysis 2. May not suppress whirl due to non-bearing causes	Used as standard design by some manufacturers
Hydrostatic	1. Wide range of design parameter 2. Moderate cost 3. Good load capacity of low speeds	1. Poor damping at critical speeds 2. Requires careful design 3. Requires high pressure lubricant supply	Generally high stiffness properties used for high precision rotors

Table 6d Nonfixed Pad Journal Bearing

Bearing Type	Advantages	Disadvantages	Comments
Tilting Pad	1. Will not cause whirl (no cross-coupling) 2. Wide range of design parameters 3. Original cost about the same as other bearings	1. High replacement cost 2. Requires careful design 3. Poor damping at critical speeds 4. Hard to determine actual clearances 5. High horsepower loss	Widely used bearing to stabilize machines with subsynchronous non-bearing excitations